Journal of Flow Chemistry (2024) 14:23–31
https://doi.org/10.1007/s41981-023-00305-w

COMMUNICATIONS

Continuous flow synthesis of *meso*-substituted porphyrins with inline UV–Vis analysis

Firdaus Parveen[1] · Henry J. Morris[1] · Harvey West[1] · Anna G. Slater[1]

Received: 1 November 2023 / Accepted: 26 December 2023 / Published online: 15 January 2024

Abstract

Porphyrin derivatives have found diverse applications due to their attractive photophysical and catalytic properties, but remain challenging to synthesize, particularly at scale. Porphyrin synthesis thus stands to benefit from the more controlled environment, opportunities for efficient optimization, and potential for scale-up available in flow. Here, we have transferred Lindsey porphyrin synthesis into flow, enabling controlled timing for oxidation and neutralization steps and real time monitoring of the reaction mixture with inline UV–Vis analysis. For tetraphenyl porphyrin (TPP), inline UV–Vis showed the presence of protonated TPP, formed due to residual acid. Thus, inline monitoring allowed optimization of the neutralization step to improve yield. Three further porphyrin substrates were produced in flow; in two cases, the yield from inline UV was significantly higher than the yield from post-purification, identifying further yield losses that could be recovered by modifying the purification step. The workflow presented here can be adapted to multiple substrates to systematically optimise porphyrin yield, reducing the time needed to develop scalable routes to these valuable compounds.

Highlights

- Four *meso*-substituted porphyrins are formed via a continuous flow process incorporating condensation, oxidation, and neutralization.
- Inline UV–Vis is used to identify the formation of unwanted protonated porphyrin and to optimise the neutralization step.
- Monitoring yield via inline UV–Vis highlights yield losses during work-up, highlighting the need for improved purification processes for less stable substrates.

Keywords Porphyrins · Continuous flow synthesis · Inline UV–vis analysis

Introduction

Porphyrins are heterocyclic macrocycles with remarkable electro-, photo- and bio-chemical properties that have consequently found applications in many settings [1]. For example, porphyrins have been used as catalysts [2, 3], sensors [4], photo dynamic therapy agents [5], non-linear optic materials [6], in dye-sensitized solar cells [7], and in molecular electronics [8, 9]. In particular, tetra-aryl *meso*-substituted porphyrins offer high chemical and thermal stability, can undergo various chemical transformations [10], and have been used as a versatile scaffold to achieve many functional architectures [11, 12].

Despite this promise, the use of porphyrins in real-world applications is limited by their challenging synthesis. Porphyrin synthesis is low-yielding, performs better at low concentrations, and needs to be optimized for each aldehyde substrate, requiring large amounts of solvent per mole of product [13]. Furthermore, synthesis of a given porphyrin can be subject to significant batch-to-batch variability, making optimization as well as subsequent purification both time- and resource-intensive.

Firdaus Parveen and Henry J. Morris contributed equally to this work.

✉ Anna G. Slater
anna.slater@liverpool.ac.uk

[1] Department of Chemistry and Materials Innovation Factory, University of Liverpool, Liverpool L69 3BX, UK

The synthesis of porphyrins has been extensively studied in order to overcome these challenges. Many approaches exist, e.g., tetramerization of mono-pyrrole or coupling of dipyrromethane units, the approach chosen depending on the desired porphyrin scaffold and functionality [13, 14].

The synthesis of a *meso*-porphyrin was first reported in 1935 by Rothemund: pyrrole, benzaldehyde, and pyridine were heated in a sealed tube reactor to obtain 10% yield of tetraphenyl porphyrin (TPP) [15, 16]. Later, Adler and Longo's method of refluxing equimolar pyrrole and benzaldehyde in propionic acid was developed, improving the yield of TPP to 20% [17, 18]. However, such harsh conditions are unsuitable for porphyrins with sensitive functional groups, and tar forms during the reaction that can be challenging to separate if the crystalline porphyrin does not precipitate out.

Later, Lindsey reacted pyrrole and benzaldehyde at room temperature in the presence of acid to reversibly form tetrapyrrolic porphyrinogen (Scheme 1) [19, 20]. To drive the reaction forward and break the equilibrium, porphyrinogen was irreversibly oxidised to porphyrin using 2,3-dichloro-5,6-dicyanobenzoquinone (DDQ) or p-chloranil [21]. Lindsey examined 45 different acids to optimize this milder process, giving yields from 1–50% [19, 22]. Reaction concentration was found to be a key parameter; the optimal condition was established to be 0.01 M. Higher concentrations resulted in formation of polymer (polypyrrylmethanes); lower concentrations resulted in the formation of oligomers with insufficient repeating units for cyclization to porphyrin [13, 23].

The flexibility and broad scope of the Lindsay method has led to its wide-spread use for porphyrin synthesis, but several challenges remain. Yields remain low due to the presence of multiple competing side reactions, as reported across a wide range of modifications to the method; i.e., the use of ionic liquids (15% yield) [24], Lewis acids (23% yield) [25], clay (20% yield), mixed solvent systems (45% yield) [26], microwave synthesis (24% yield) [27], and transition metal ion templating (44% yield) [28] all give yields that are similar to that reported for the original conditions (trifluoroacetic acid, typically 38%) [19].

Furthermore, these modified methods are generally reported for specific substrates; a strategy for systematic optimization that could be applied to any aldehyde substrate is lacking. Reported optimal reaction times for different substrates vary from seconds (e.g., for 1-anthracenecarbaldehyde) [29] to hours (e.g., for 4-methoxybenzaldehyde) [22, 30]; it is challenging to identify the maximum yield of porphyrinogen over these timescales, and thus the optimal time for oxidation. Most methods still require high dilution, limiting scale up [10, 31]. Finally, if insufficient base is used, porphyrins are readily protonated, reducing yields via the formation of protonated porphyrin.

Reaction monitoring has been previously used to track the reversible chemistry of porphyrinogen formation and to determine the optimal time to oxidise the reaction [32]. However, reaction monitoring becomes difficult for rapid reactions under batch conditions and is time-consuming to perform accurately. As such, the synthesis of porphyrins seems an ideal candidate for study under continuous flow conditions.

Flow chemistry offers the advantage of controlling the reaction parameters, residence time, mixing, and heat and mass transfer, as well as providing safe handling of toxic reagents, multi-step synthesis via telescoping, automation opportunities, and routes to scale up [33–35]. Robust control of heat and mass transfer could enable a greater degree of control over the reversible porphyrinogen formation as compared to batch, and at-line [36] and inline analytical tools [37, 38] provide access to reaction monitoring even at very short times post-mixing.

Momo et al. reported the first continuous flow synthesis of porphyrin adapting the Gonsalves conditions [39] using propionic acid and nitrobenzene as solvent, carrying out the condensation and oxidation in a single coil. Optimization of the reaction led to a TPP yield of 31% at 140 °C with a residence time of 27 min. A range of aromatic aldehydes were investigated and yields of 9–39% were achieved [40]. The flow process is scalable, but not compatible with reactants or products that are sensitive to acids or elevated temperature; furthermore, the concurrent formation and oxidation to porphyrin limits opportunities to study and optimise each step of the process.

Here, we have adapted Lindsey porphyrin synthesis to flow to study the condensation and oxidation steps independently, aiming to maximize the yield of porphyrinogen and improve selectivity. We compared the synthesis of porphyrin via two flow processes: (1) a semi-continuous process, with condensation of pyrrole and aldehyde in one reactor, oxidation of porphyrinogen in a second reactor, and neutralization of reaction mixture in batch; (2) a fully continuous process where the neutralization step was moved into flow in a third reactor, and the flow pathway was augmented with real time monitoring by UV–Vis spectroscopy.

First, the semi-continuous formation of TPP was subjected to an initial optimization to screen residence time, concentration, equivalents of TFA, and temperature of the first step. Then, the fully continuous method was developed to include inline UV analysis, revealing that the neutralization step was contributing to reduced yields. With this corrected, the scope of the process was studied on both platforms using three aldehydes with sensitive functional groups (thio, ether and silyl alkyne). Here, discrepancies between the inline yield and isolated yield revealed that degradation was likely occurring

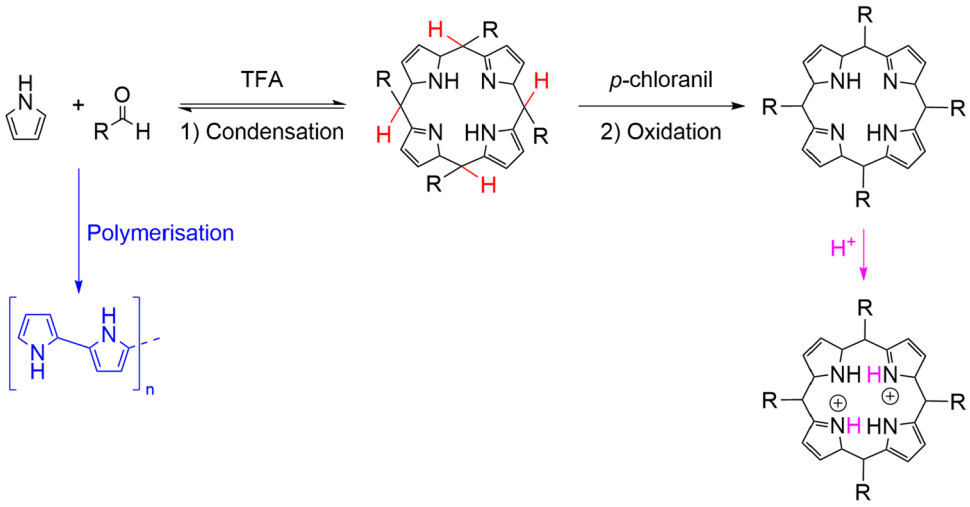

Scheme 1 Steps involved in the synthesis of porphyrin; possible side-products include polypyrrole and protonated porphyrin, indicated with blue and pink respectively

during purification, demonstrating the value of inline analysis and the fully continuous system. As such, we have developed a flow process that can be used to rapidly optimize porphyrin yield, and that has scope for further augmentation to enable kinetic monitoring and automated optimization.

Results and discussion

Semi-continuous flow synthesis of porphyrin

The semi-continuous flow pathway was set up as described below (Fig. 1). Briefly, two reactors for condensation (reactor 1) and oxidation (reactor 2) were set up in series; the reaction mixture from reactor 2 was collected and quenched with triethylamine. For initial screening of parameters tetraphenyl porphyrin (TPP) was used as a model compound [41].

The effect of reactant concentration, residence time, acid equivalents, and the temperature of coil 1 on TPP yield was studied in an initial optimization (Table 1). Equivalents of pyrrole and benzaldehyde were maintained at 1:1 and reaction temperature for the oxidation step was fixed at 50 °C [21]. A detailed description of reaction parameters and reactor setup is in section S1.2 of SI.

A decrease in porphyrin yield was observed with increase in concentration from 0.018 M to 0.025 M (Table 1, entries 1, 2, and 3, 38–23%), in line with observations that high dilution conditions minimize the polymerization of pyrrole under batch conditions [21]. Increasing residence time (entries 2, 4, 5; 27–33%) and reaction temperature (entries 2, 6; 31–35%) led to small improvements in the porphyrin yield. However, further increasing the temperature to 50 °C had a negative effect on the yield of porphyrin (entry 7; 24%). The optimum concentration of TFA was found to be

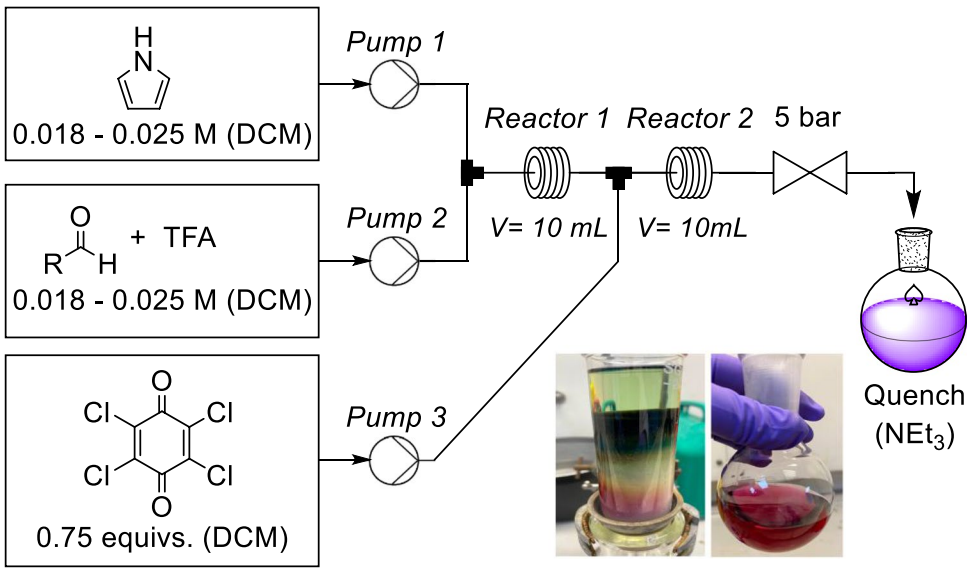

Fig. 1 Semi-continuous reaction pathway for porphyrin synthesis and batch neutralization

Table 1 Optimization reactions of TPP under continuous flow using TFA

Entry	Reagent Concentration (M)	Residence Time (mins)	Reactor 1 T (°C)	Equivalents of TFA	Yield (%)
1	0.018	20	25	2	38
2	0.02	20	25	2	31
3	0.025	20	25	2	23
4	0.02	17	25	2	27
5	0.02	25	25	2	33
6	0.02	20	35	2	35
7	0.02	20	50	2	24
8	0.02	20	25	2.25	38
9	0.02	20	25	2.5	42

*Reactor 2: Temperature 50 °C

2.5 equivalents (Table 1, entries 2,8 and 9; 31–42%), giving a maximum porphyrin yield of 42%.

In these experiments, yields ranging between 23–42% were observed. However, during purification, a green colour was observed on the silica plug, indicating the presence of protonated porphyrin, and suggesting that the yield of porphyrin could be increased if the neutralization step was improved. Indeed, the global optimum of the reaction may be outside the parameters studied; here, a full design of experiments (DoE) approach would be informative [42–44]. However, to achieve robust DoE, the above set-up requires inline analysis and better control over the final neutralization step. Thus, the flow pathway was modified to include flow neutralization, and to integrate inline UV–Vis spectroscopy for real time monitoring of the reaction mixture.

Continuous synthesis and neutralization of porphyrin, incorporating real time monitoring of reaction mixture using inline UV–Vis spectrometer

The reactor set up was therefore modified to neutralize the reaction mixture in a third reactor, and to include inline UV–Vis (Fig. 2). The detailed reactor set up is described in S1.3 of the SI.

Porphyrins are highly conjugated π-electron systems with characteristic absorption bands in the near-ultraviolet and visible regions. The transition from the ground state to the second excited state results in an intense Soret, or B, band in the region of 380–500 nm; the transition of electron from ground to first excited state results in a weaker Q

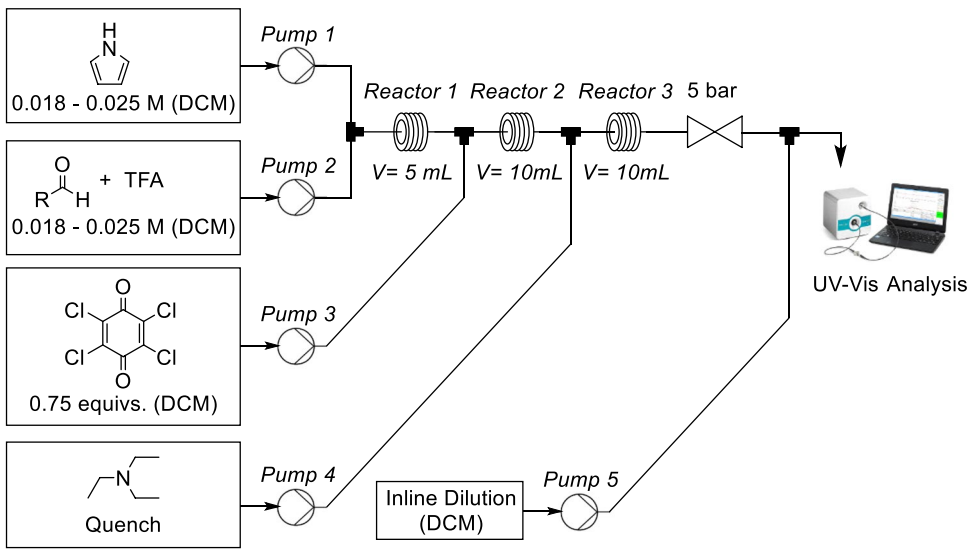

Fig. 2 Reactor design for continuous synthesis of porphyrin with real time UV–Vis analysis

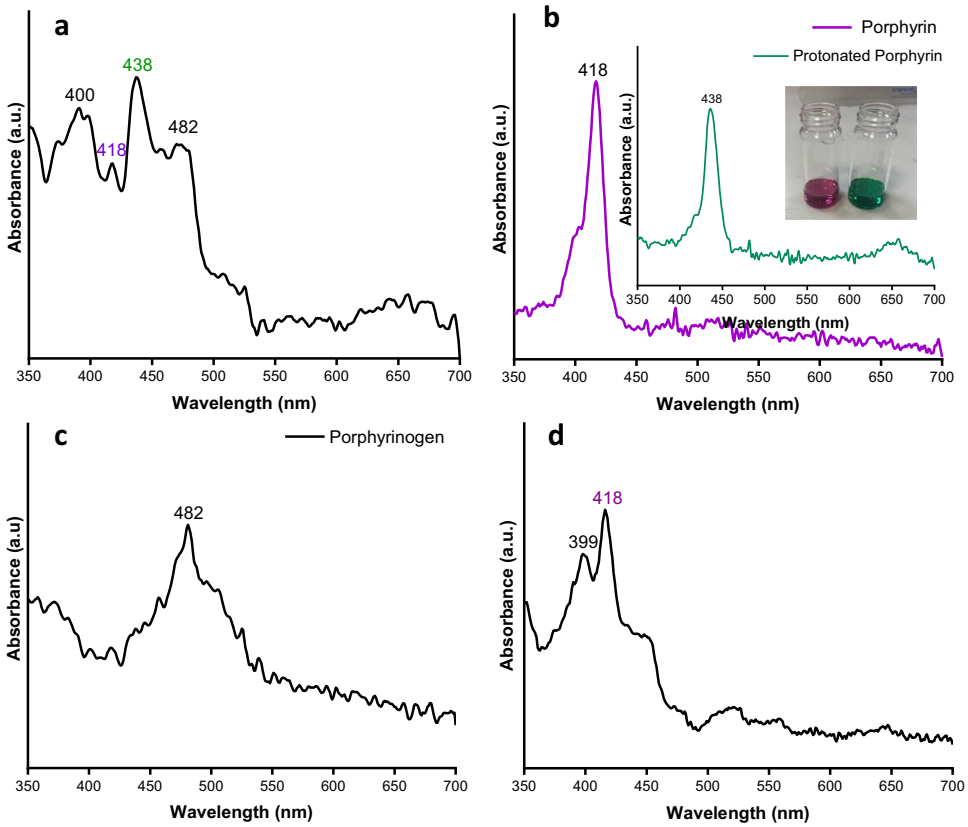

Fig. 3 **a** UV–Vis spectrum of reaction under conditions described above and with solution collected after neutralization with 0.9 µL/mL base **b** Reference UV–Vis spectra of porphyrin and protonated porphyrin; **c** UV–Vis spectrum of porphyrinogen as collected after reactor 1; **d** UV–Vis spectrum of reaction mixture after complete inline neutralization with 100 µL/mL

band in the region of 500–750 nm [45]. Inline UV–Vis is thus an ideal diagnostic tool for porphyrin yield. The Soret band is affected by concentration: TPP at higher concentration (370–180 µg/mL) had an intense peak at 399/400 nm, whereas diluting the solution (90–9 µg/mL) shifted the intense peak to 417 with a shoulder at 399 (SI 1.5) [46].

First, TPP was formed using the most promising conditions from Table 1: 0.02 M pyrrole and benzaldehyde, 2.5 equivalent of TFA, 20 min residence time, 25 °C temperature in reactor 1, 10 min residence time, 50 °C temperature in reactor 2, and neutralization in reactor 3 at 30 °C with 3.3 min residence time. The UV spectrum of the inline neutralized reaction stream at outlet showed peaks at 418 nm, 438 nm and 482 nm (Fig. 3a). The peaks at 418 nm and 438 nm correspond to porphyrin and protonated porphyrin respectively, as confirmed via reference to standards carried out in the same flow cell (Fig. 3b). The peak observed at 482 nm corresponds to porphyrinogen; the reference spectrum collected at the outlet of reactor 1 is shown in Fig. 3c.

The presence of all three species in the reaction mixture collected at the end of reactor 3 (Fig. 3a) demonstrated that protonation of the porphyrin due to incomplete neutralization of the reaction was reducing the overall yield. The major peak observed was 438 nm, indicating that residual acid was protonating the porphyrin. The presence of a peak at 482 nm, corresponding to porphyrinogen, also indicated incomplete oxidation of porphyrinogen to porphyrin under these conditions.

It is thus important to optimize the concentration of base required to completely neutralize the residual acid and increase the yield of porphyrin. Thus, the concentration of base was varied from 0.9 µL/mL to 100 µL/mL, with all other reaction parameters kept as specified above; briefly, 0.02 M pyrrole and benzaldehyde, 2.5 equivalent of TFA, 20 min residence time, 25 °C temperature in reactor 1, 10 min residence time, 50 °C temperature in reactor 2, and neutralization in reactor 3 at 30 °C with 3.3 min residence time. The spectrum reported in Fig. 3d is the result at 100 µL/mL and shows the disappearance of protonated porphyrin peak. In this case, porphyrinogen was not observed.

The possibility of the presence of other species was considered. Chloranil and its complex with triethylamine display peaks in the UV at 295 nm and 319 nm respectively (S1.6), which is sufficiently distant from the peak at 418 nm for porphyrin quantification.

Comparison of two processes for the synthesis of functionalized porphyrins

To verify the improvements of the fully continuous process, functionalized porphyrins with thio (5,10,15,20-tetrakis(4-(methylthio)phenyl)porphyrin), ether

Table 2 Comparison of two different processes for the synthesis of functionalized porphyrin

Substrate scope	% isolated yield (semi-continuous process)[a]		% analytical yield (fully continuous process)[b]	
	TFA (equivalents)			
	(2.0)	(2.5)	(2.0)	(2.5)
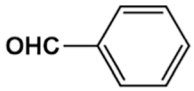	31	42	35	43
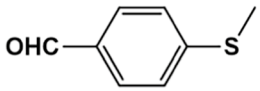	19	11	32	29
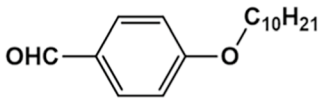	18	15	21	29
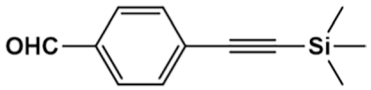	21	19	30	45

a) Yields are calculated after silica plug purification.

b) Yields are calculated by UV-Vis spectroscopy employing the external calibration curve for functionalized porphyrin as reported in SI, S1.4

(5,10,15,20-tetrakis(4-(decyloxy)phenyl)porphyrin), and alkynyl silyl (5,10,15,20-tetrakis(4-(trimethylsilyl)ethynyl) phenyl)porphyrin) functional groups were trialled in both the semi-continuous and continuous set-up. Calibration curves (S1.4) were carried out for each substrate to use inline UV detection to establish analytical yields for the fully continuous process. For the semi-continuous process yields were obtained via isolation and weighing of the porphyrin post-purification, and thus are subject to losses during work-up and purification.

In the case of TPP (benzaldehyde; Table 2, entry 1) the yields obtained from both processes were comparable. However, thio (Table 2, entry 2), ether (Table 2, entry 3), and alkynyl silyl (Table 2, entry 4) functionalities showed substantial difference in the yields obtained from two different processes. The isolated yields obtained during the batch neutralization in semi-continuous mode were found to be much lower compared to the analytical yields obtained from the fully continuous synthesis, except for the ether substituted porphyrin with 2 equivalents of acid used. This can be attributed to the instability of the porphyrins appended with thio, ether, and alkynyl silyl functional groups, incomplete neutralization of porphyrin, and/or yield losses during silica plug purification.

In the case of the fully continuous synthesis, higher equivalents of acid resulted in higher yield for three of the porphyrins, except for the thio-substituted porphyrin. On the contrary, yields obtained in the semi-continuous process were higher with lower equivalents of acid. We hypothesize that the presence of higher concentrations of acid may degrade less stable porphyrin derivatives, especially if insufficient base is used for neutralization. Here, inline purification methods would be beneficial to achieve high yields of porphyrin compounds appended with sensitive functional groups, especially coupled with automated optimization approaches to efficiently identify optimal quantities of base.

Conclusion

We have developed two processes, semi-continuous and continuous, for the synthesis of *meso*-porphyrin derivatives via the Lindsay method. Continuous flow synthesis with inline UV–Vis analysis offers the advantage of real time monitoring of the reaction steady state, the reaction mixture, and the porphyrin yield, giving better understanding of the process including where yield losses are occurring. In case of TPP, similar yields were obtained from both the semi-continuous and continuous process. However, in case of functionalized porphyrins with thio, ether, and alkynyl silyl groups, the analytical yields from continuous mode with inline UV were higher than the isolated yields from semi-continuous mode, which employed batch neutralization. The lower yields observed in the semi-continuous process may be due to the degradation of the less stable porphyrin derivatives under incomplete neutralization conditions, or losses during work-up and purification. Hence, inline UV analysis proved to be essential to improve the process by actual determination of steady state, optimising the base for complete neutralization of acid, and indicating

what the achievable yields are immediately following oxidation. In future, this system will be augmented with in-line purification and modified to allow autonomous optimization, allowing the rapid exploration of process space for a range of porphyrin precursors, ultimately improving selectivity, yield, and scalability of these important molecules.

Supplementary Information The online version contains supplementary material available at https://doi.org/10.1007/s41981-023-00305-w.

Acknowledgements AGS thanks the Royal Society and the Engineering and Physical Sciences Research Council (EPSRC) for a Royal Society-EPSRC Dorothy Hodgkin Fellowship (DH150156), and the Royal Society for a University Research Fellowship (URF\R1\201168) and a Research Grant (RSG\R1\180357) that supported this work. HM and AGS thank the University of Liverpool Leverhulme Centre for Functional Materials Design for a PhD studentship. This work made use of equipment from the Analytical Services/Department of Chemistry at the University of Liverpool, as well as shared equipment at the Materials Innovation Factory (MIF) created as part of the UK Research Partnership Innovation Fund (Research England) and co-funded by the Sir Henry Royce Institute. AGS, FP, and HW thank the University of Liverpool for providing funding to accomplish this work, including a PhD studentship (HW). AGS would like to thank Professor Harris Makatsoris (King's College London) and the EPRSC Directed Assembly Network for supporting a visit to his labs at Brunel University to carry out preliminary porphyrin flow synthesis reactions assisted by Dr Leonid Paramonov. All authors would like to acknowledge Glyn Connolly and Steven Robinson for their support in collecting MALDI data at the Material Innovation Factory.

Author contribution Conceptualisation, supervision, and funding acquisition was carried out by AGS. Experiments were carried out by FP and HM, who both led the methodology design; HM led the work on the semi-continuous process, and FP led the work on the fully continuous process equipped with UV detection. All authors contributed to experimental design, analytical measurement, and interpretation of results. FP produced the first draft and all authors contributed to the final manuscript.

Data availability All the research data generated from this study are contained within the manuscript and supporting information.

Declarations

Conflict of interest On behalf of all authors, the corresponding author states that there is no conflict of interest.

References

1. Adler AD (1973) The chemical and physical behavior oe porphyrin compounds and related structures. Ann NY Acad Sci 206(1):5–761
2. Srour H, Le Maux P, Simonneaux G (2012) Enantioselective manganese-porphyrin-catalyzed epoxidation and c-h hydroxylation with hydrogen peroxide in water/methanol solutions. Inorg Chem 51:5850–5856. https://doi.org/10.1021/ic300457z
3. Yang H, Shi R, Shang L, Zhang T (2021) Recent advancements of porphyrin-like single-atom catalysts: Synthesis and applications. Small Struct 2. https://doi.org/10.1002/sstr.202100007
4. Capuano R, Pomarico G, Paolesse R, Di Natale C (2015) Corroles-porphyrins: A teamwork for gas sensor arrays. Sensors (Basel) 15:8121–8130. https://doi.org/10.3390/s150408121
5. Tian J, Huang B, Nawaz MH, Zhang W (2020) Recent advances of multi-dimensional porphyrin-based functional materials in photodynamic therapy. Coord Chem Rev 420:213410. https://doi.org/10.1016/j.ccr.2020.213410
6. Bao C, Li Y, Li Y, Si Z, Zhang Y, Chen C, Wang L, Duan Q (2021) A series of asymmetric and symmetric porphyrin derivatives: One-pot synthesis, nonlinear optical and optical limiting properties. New J Chem 45:16030–16038. https://doi.org/10.1039/D1NJ02632A
7. Li LL, Diau EW (2013) Porphyrin-sensitized solar cells. Chem Soc Rev 42:291–304. https://doi.org/10.1039/c2cs35257e
8. Paolesse R, Nardis S, Monti D, Stefanelli M, Di Natale C (2017) Porphyrinoids for chemical sensor applications. Chem Rev 117:2517–2583. https://doi.org/10.1021/acs.chemrev.6b00361
9. Martynov AG, Safonova EA, Tsivadze AY, Gorbunova YG (2019) Functional molecular switches involving tetrapyrrolic macrocycles. Coord Chem Rev 387:325–347. https://doi.org/10.1016/j.ccr.2019.02.004
10. Lindsey JS (2010) Synthetic routes to meso-patterned porphyrins. Acc Chem Res 43:300–311. https://doi.org/10.1021/ar900212t
11. Ding G, Han S-T, Kuo C-C, Roy VAL, Zhou Y (2023) Porphyrin-based metal–organic frameworks for neuromorphic electronics. Small Struct 4:2200150. https://doi.org/10.1002/sstr.202200150
12. He T, Zhao Z, Liu R, Liu X, Ni B, Wei Y, Wu Y, Yuan W, Peng H, Jiang Z, Zhao Y (2023) Porphyrin-based covalent organic frameworks anchoring au single atoms for photocatalytic nitrogen fixation. J Am Chem Soc 145:6057–6066. https://doi.org/10.1021/jacs.2c10233
13. Koifman OI, Ageeva TA (2022) Main strategies for the synthesis of meso-arylporphyrins. Russ J Org Chem 58:443–479. https://doi.org/10.1134/s1070428022040017
14 Vicente MdGH, Smith KM (2014) Syntheses and functionalizations of porphyrin macrocycles. Curr Org Synth 11(1):3–28
15. Rothemund P (1935) Formation of porphyrins from pyrrole and aldehydes. J Am Chem Soc 57:2010–2011. https://doi.org/10.1021/ja01313a510
16. Rothemund P, Menotti AR (1941) Porphyrin studies. Iv.1 the synthesis of α, β, γ, δ-tetraphenylporphine. J Am Chem Soc 63:267–270. https://doi.org/10.1021/ja01846a065
17. Adler AD, Longo FR, Finarelli JD, Goldmacher J, Assour J, Korsakoff L (1967) A simplified synthesis for meso-tetraphenylporphine. J Org Chem 32:476–476. https://doi.org/10.1021/jo01288a053
18. Adler AD, Longo FR, Shergalis W (1964) Mechanistic investigations of porphyrin syntheses. I. Preliminary studies on ms-tetraphenylporphin. J Am Chem Soc 86:3145–3149

19. Geier GR, Ciringh Y, Li F, Haynes DM, Lindsey JS (2000) A survey of acid catalysts for use in two-step, one-flask syntheses of meso-substituted porphyrinic macrocycles. Org Lett 2:1745–1748. https://doi.org/10.1021/ol005917h
20. Wagner RW, Li F, Du H, Lindsey JS (1999) Investigation of cocatalysis conditions using an automated microscale multireactor workstation: Synthesis of m eso-tetramesitylporphyrin. Org Process Res Dev 3:28–37
21. Lindsey JS, Schreiman IC, Hsu HC, Kearney PC, Marguerettaz AM (1987) Rothemund and adler-longo reactions revisited: Synthesis of tetraphenylporphyrins under equilibrium conditions. J Org Chem 52:827–836. https://doi.org/10.1021/jo00381a022
22. Geier GR, Lindsey JS (2002) Effects of diverse acid catalysts on the reaction course in the two-step one-flask synthesis of meso-tetraphenylporphyrin. J Porphyrins Phthalocyanines 06:159–185. https://doi.org/10.1142/S1088424602000208
23. Maddison DS, Unsworth J (1989) Optimization of synthesis conditions of polypyrrole from aqueous solutions. Synth Met 30:47–55. https://doi.org/10.1016/0379-6779(89)90640-1
24. Kitaoka S, Nobuoka K, Hirakawa R, Ihara K, Ishikawa Y (2013) Porphyrin preparation in acidic ionic liquids. Chem Lett 42:1397–1399. https://doi.org/10.1246/cl.130662
25. Geier GR, Lindsey JS (2004) Effects of aldehyde or dipyrromethane substituents on the reaction course leading to meso-substituted porphyrins. Tetrahedron 60:11435–11444. https://doi.org/10.1016/j.tet.2004.09.081
26. Sun Z, She Y, Cao M, Zhou Q, Lu X, Zhang S (2013) Synthesis of substituted meso-tetraphenylporphyrins in mixed solvent systems. ARKIVOC 3:389–400
27. Nascimento BFO, Piñeiro M, Gonsalves AMAR, Silva MR, Beja AMM, Paixão JA (2007) Microwave-assisted synthesis of porphyrins and metalloporphyrins: A rapid and efficient synthetic method. J Porphyrins Phthalocyanines 11:77–84
28. Kumar A, Maji S, Dubey P, Abhilash GJ, Pandey S, Sarkar S (2007) One-pot general synthesis of metalloporphyrins. Tetrahedron Lett 48:7287–7290. https://doi.org/10.1016/j.tetlet.2007.08.046
29. Tohara A, Sato M (2007) An improved synthesis of meso-tetraanthrylporphyrin by a kinetically controlled lindsey reaction. J Porphyrins Phthalocyanines 11:513–518. https://doi.org/10.1142/S108842460700059X
30. Kim JB, Leonard J, Longo FR (1972) A mechanistic study of the synthesis and spectral properties of meso-tetraarylporphyrins. J Am Chem Soc 94(11):3986–3992
31. Smith KM (2016) Development of porphyrin syntheses. New J Chem 40:5644–5649. https://doi.org/10.1039/c6nj00820h
32. Geier Iii GR, Lindsey JS (2001) Investigation of porphyrin-forming reactions. Part 1. Pyrrole + aldehyde oligomerization in two-step, one-flask syntheses of meso-substituted porphyrins. J Chem Soc Perkin Trans 2, 677–686. https://doi.org/10.1039/B009088N
33 Jas G, Kirschning A (2003) Continuous flow techniques in organic synthesis. Chem A Eur J 9:5708–5723. https://doi.org/10.1002/chem.200305212
34. McQuade DT, Seeberger PH (2013) Applying flow chemistry: Methods, materials, and multistep synthesis. J Org Chem 78:6384–6389
35. He C, Zhang C, Bian T, Jiao K, Su W, Wu K-J, Su A (2023) A review on artificial intelligence enabled design, synthesis, and process optimization of chemical products for industry 4.0. Processes 11:330
36. Jones CD, Kershaw Cook LJ, Marquez-Gamez D, Luzyanin KV, Steed JW, Slater AG (2021) High-yielding flow synthesis of a macrocyclic molecular hinge. J Am Chem Soc 143:7553–7565. https://doi.org/10.1021/jacs.1c02891
37. Lauterbach F, Abetz V (2020) Continuous kinetic sampling of flow polymerizations via inline uv–vis spectroscopy. Macromol Rapid Commun 41:2000029. https://doi.org/10.1002/marc.202000029
38. Van Herck J, Junkers T (2022) Rapid kinetic screening via transient timesweep experiments in continuous flow reactors. Chemistry-Methods 2:e202100090. https://doi.org/10.1002/cmtd.202100090
39 Gonsalves AMdAR, Varejão JMTB, Pereira MM (1991) Some new aspects related to the synthesis of meso-substituted porphyrins. J Heterocycl Chem 28:635–640. https://doi.org/10.1002/jhet.5570280317
40. Momo PB, Bellete BS, Brocksom TJ, de Souza ROMA, de Oliveira KT (2015) Exploiting novel process windows for the synthesis of meso-substituted porphyrins under continuous flow conditions. RSC Adv 5:84350–84355. https://doi.org/10.1039/c5ra16962c
41. Lindsey JS, MacCrum KA, Tyhonas JS, Chuang YY (1994) Investigation of a synthesis of meso-porphyrins employing high concentration conditions and an electron transport chain for aerobic oxidation. J Org Chem 59:579–587. https://doi.org/10.1021/jo00082a014
42. Taylor CJ, Baker A, Chapman MR, Reynolds WR, Jolley KE, Clemens G, Smith GE, Blacker AJ, Chamberlain TW, Christie SDR, Taylor BA, Bourne RA (2021) Flow chemistry for process optimisation using design of experiments. J Flow Chem 11:75–86. https://doi.org/10.1007/s41981-020-00135-0
43. Echtermeyer A, Amar Y, Zakrzewski J, Lapkin A (2017) Self-optimisation and model-based design of experiments for developing a c–h activation flow process. Beilstein J Org Chem 13:150–163. https://doi.org/10.3762/bjoc.13.18
44. Gioiello A, Mancino V, Filipponi P, Mostarda S, Cerra B (2016) Concepts and optimization strategies of experimental design in continuous-flow processing. J Flow Chem 6:167–180. https://doi.org/10.1556/1846.2016.00012
45. Rita G (2012) in *Macro to nano spectroscopy*, ed. Jamal, U., IntechOpen, Rijeka. p. Ch. 6. https://doi.org/10.5772/38797
46. Dallagnol JCC, Ducatti DRB, Barreira SMW, Noseda MD, Duarte MER, Gonçalves AG (2014) Synthesis of porphyrin glycoconjugates bearing thiourea, thiocarbamate and carbamate connecting groups: Influence of the linker on chemical and photophysical properties. Dyes Pigm 107:69–80. https://doi.org/10.1016/j.dyepig.2014.03.029

Firdaus Parveen is Research Coordinator and Flow Centre Manager in the Slater Group at the University of Liverpool. Firdaus Parveen received her Master's degree in Chemistry (2011) and Doctorate in Chemical Engineering (2017) from the Indian Institute of Technology (IIT) Delhi, India. Following postdoctoral positions at USASK, Canada, IIT Delhi, and Imperial College London, Firdaus joined the University of Liverpool in 2021 as PDRA before taking up her current position in 2023. She has gained advanced experience of continuous flow chemistry, building flow equipment, automated reactions, and heterogenous catalysis.

Henry Morris is currently Health & Safety Officer in Chemistry at the University of Liverpool. Henry received an MChem degree from the University of Leicester, which included a placement year at Hexcel Composites, before moving to the University of Liverpool for a PhD in the Slater Group supported by the Leverhulme Research Centre for Functional Materials Design. Henry's PhD work compared continuous flow and batch methodologies for a range of macrocyclic and organic cage syntheses and included a 12-month postgraduate research associate position in collaboration with industry and funded by an EPSRC IAA grant.

Harvey West graduated in 2023 from the University of Liverpool with an MChem degree. He has recently developed a strong interest in the deployment of enabling technologies and machine learning in the lab and aims to apply these in the pursuit of synthesising novel macrocyclic targets and delivering more sustainable chemical processes. Harvey's PhD commenced in Oct 2023 within the Slater group, co-supervised by Prof Andy Cooper (Liverpool) and Prof Richard Bourne (Leeds). He has two main goals, the development of novel techniques for self-optimised flow chemistry, and testing and cataloguing the properties and potential applications of supramolecular systems.

Anna Slater graduated from the University of Nottingham with a PhD in Supramolecular Chemistry (2011). After PDRA positions in surface self-assembly and porous molecular materials Anna took up a Royal Society-EPSRC Dorothy Hodgkin Fellowship in 2016 and a Royal Society University Research Fellowship in 2021. She was promoted to Senior Lecturer (proleptic) in Oct 2021, and awarded a Personal Chair in Oct 2022. Her research interests span flow synthesis, materials science, supramolecular self-assembly, and enabling technology for sustainable chemistry.